



Cite this: *RSC Appl. Polym.*, 2025, **3**, 173

## Water-harvesting polymer coatings for plant leaves†

Roland Milatz,<sup>a</sup> Carmen Reink,<sup>a</sup> Tomas E. van den Berg,<sup>b</sup> Joost Duvigneau,<sup>\*a</sup> G. Julius Vancso <sup>a</sup> and Frederik R. Wurm <sup>b</sup>

Climate change-induced water scarcity threatens global plant life and agricultural productivity. Here, we present a novel atmospheric water harvesting (AWH) coating designed to alleviate heat and dry stress potentially. This polymer coating utilizes block copolymers carrying catechol-anchoring groups, specifically poly(dopamine methacrylamide) (PDOMA), to adhere to plant leaves. As a hydrophilic block, either poly((oligoethylene glycol) methacrylate) (POEGMA) or the thermoresponsive block poly(*N*-isopropylacrylamide) (PNIPAM) was used, which can adsorb water from the air during cooler periods in its hydrophilic state. As the temperature increases above the lower critical solution temperature (LCST) of PNIPAM, the polymer transitions to a hydrophobic state, releasing the captured water to the leaf surface. We synthesized PNIPAM-*b*-PDOMA copolymers *via* RAFT polymerization and confirmed their composition (IR, <sup>1</sup>H NMR and <sup>1</sup>H DOSY NMR spectroscopy) with a cloud point temperature of  $33 \pm 1$  °C. The coatings were applied to model substrates (SiO<sub>2</sub>, polyethylene) and corn leaves. Compared to uncoated controls, coated substrates demonstrated a substantial increase in water uptake from humid air, absorbing up to 50 wt% of the coating's weight. The coating's adherence and thermoresponsive behavior were confirmed on corn leaves through contact angle measurements, showing a shift from hydrophilic ( $29 \pm 3$ °) below the LCST to hydrophobic ( $80 \pm 2$ °) above the LCST, closer to the native, hydrophobic leaf ( $110 \pm 10$ °). Crucially, photosynthesis induction experiments revealed that the coating did not negatively impact the plant's natural photosynthetic processes. This study establishes a promising copolymer platform for developing AWH coatings to support plants in the face of increasing drought conditions.

Received 9th August 2024,  
Accepted 6th November 2024  
DOI: 10.1039/d4lp00249k  
rsc.li/rscapplpolym

## 1. Introduction

Climate change brings undue stress to plants due to extreme weather conditions, such as heat waves, storms, droughts, *etc.*<sup>1</sup> Higher average temperatures in summer<sup>2</sup> as well as longer and more common heatwaves create increased dry-stress for plants and influence crop yield or contribute to forest dieback.<sup>3</sup> Several studies have demonstrated negative impact of climate change on plant growth over the past 50 years.<sup>4</sup> The yield trends of crops predict shortages for 2050 to feed the increasing world population.<sup>5</sup> For example, corn is one of the major crops (~1.2 billion metric tonnes<sup>18</sup>) produced worldwide,

which is known to be sensitive to water stress resulting in decreased production rates.<sup>3</sup> Active measures to support plants against heat-stress are urgently needed.

Generally, plants can have two types of stress: biotic and abiotic. Biotic stress comes from biological sources such as pests or fungi.<sup>6</sup> Abiotic stress is caused by physical parameters such as temperature, droughts, or floods.<sup>7</sup> These stress factors can negatively impact the development and quality of plants and crops.<sup>8</sup> Specifically, we look at alleviating stress caused by water scarcity. Water scarcity limits crop growth initially in the gas exchange and thus photosynthesis. Prolonged and intense dry-stress results in low nutrient transport in the plant.

A promising method to cope with dry-stress could be the harvesting of water from the atmosphere. To apply such a system on plants, there are several requirements to be met, which include low energy consumption, easy applicability, robustness, and stability.<sup>9</sup> Current atmospheric water harvesting (AWH) systems, which are not applied on plants, tend to fall short of these requirements. Today's systems include metal-organic frameworks (MOFs), crystalline, porous structures containing inorganic coordination centers, and organic linkers.<sup>10</sup> For example, Kim *et al.*<sup>11</sup> synthesized a

<sup>a</sup>Sustainable Polymer Chemistry, Department of Molecules and Materials, MESA+ Institute for Nanotechnology, Faculty of Science and Technology, University of Twente, Enschede, The Netherlands. E-mail: g.j.vancso@utwente.nl, j.duvigneau@utwente.nl, Frederik.wurm@utwente.nl

<sup>b</sup>Department of Integrated Devices and Systems, Faculty of Electrical Engineering, Mathematics & Computer Science, University of Twente, Enschede, 7522 NB, The Netherlands

† Electronic supplementary information (ESI) available. See DOI: <https://doi.org/10.1039/d4lp00249k>

$[\text{Zr}_6\text{O}_4(\text{OH})_4(\text{fumarate})_6]$  MOF, which is capable of functioning at ambient temperatures and low relative humidities while requiring no input of energy. Hygroscopic materials, such as salts or polymers, are another option; they are capable of capturing 5 to 6 times their weight in water.<sup>10</sup> They suffer from some drawbacks, such as deterioration over time.<sup>12</sup> Thermoresponsive polymers, such as poly(*N*-isopropylacrylamide) (PNIPAM), are also attractive materials for AWH. PNIPAM has been used in a MOF<sup>13</sup> system and a gel,<sup>14</sup> grafted onto silica gel,<sup>15</sup> or used as nanofibers<sup>16</sup> in previous studies for water harvesting.

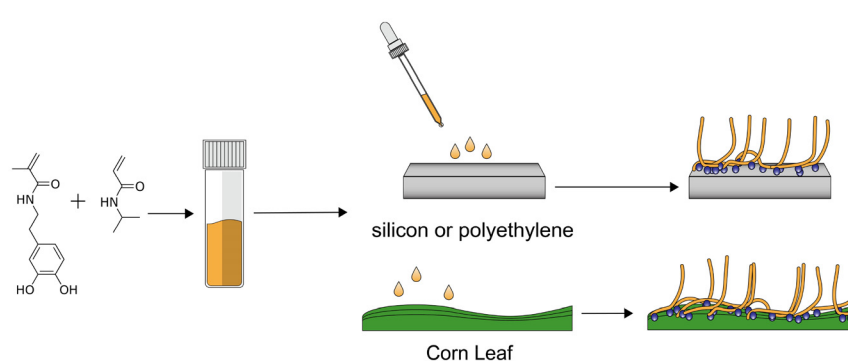
Here, we present a different approach, *i.e.* direct application of a AWH polymer coating on the leaves of living plants to harvest water from the air. We use a model system based on block copolymers, containing PNIPAM as a thermoresponsive segment and poly(dopamine methacrylamide) (PDOMA) as an adhesive block. The block copolymers are sprayed from solution on corn leaves; the system is capable of switching between hydrophilic and hydrophobic states, and demonstrates its capacity as a functional coating capable of collecting and releasing water under ambient conditions at night and day temperatures for example. PNIPAM is a well-known thermo-responsive polymer with a lower critical solution temperature (LCST) in the range of 30–40 °C, depending on its composition.<sup>17</sup> DOMA is a catechol-based, mussel-inspired adhesive monomer, capable of adhering to a variety of substrates such as polyethylene or the hydrophobic surface of leaves.<sup>19</sup> We focus on the use of a stimulus-responsive copolymer, PNIPAM-*b*-PDOMA, as a coating on corn leaves to provide an AWH system (Scheme 2). The PNIPAM-*b*-PDOMA block copolymer was synthesized using reversible addition-fragmentation chain-transfer (RAFT) polymerization and characterized using <sup>1</sup>H NMR, DOSY NMR, and GPC. First, we describe the application of the coating to a Si wafer for layer characterization using AFM. Then, we discuss using PE as a hydrophobic substrate for layer attachment. The ability of the coating to gather water from air is characterized using model PE substrates under a water vapor-saturated air stream. Finally, we apply the coating to biological corn plant leaves (Scheme 1). After application on corn leaves, plant health was monitored by measur-

ing its ability to continue supporting photosynthesis. We believe that the direct coating of living plant leaves can be an active measure against dry-stress in future agriculture and horticulture.

## 2. Results and discussion

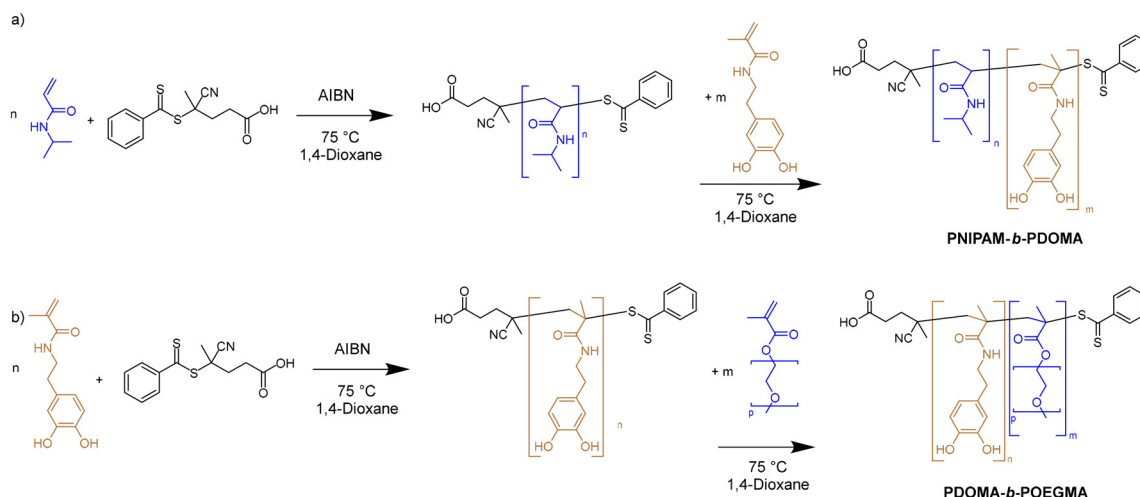
The PNIPAM-*b*-PDOMA on PDOMA-*b*-POEGMA block copolymer synthesis was adapted from previously published procedures using a NIPAM : DOMA or OEGMA : DOMA molar ratio of 14 : 1 and 0.04 eq. of 4-cyano-4-(thiobenzoylthio)pentanoic acid as the CTA with 0.008 eq. of AIBN as the respective initiator (Scheme 2).<sup>20</sup> The chemical structure of the polymers was characterized by NMR spectroscopy (Fig. S1–S3†). For the PDOMA-*b*-POEGMA polymer, we switched the addition point of OEGMA and DOMA in the procedure due to the higher viscosity of POEGMA. In the <sup>1</sup>H NMR spectra, the resonances corresponding to DOMA's aromatic ring are detected at *ca.* 6.6 ppm. The broad resonance at *ca.* 1 ppm was attributed to the methyl groups in the isopropyl head of NIPAM, whereas the tertiary carbon's protons in the isopropyl group were detected at *ca.* 3.9 ppm. The composition of the copolymer was calculated by comparison of the integrals of the methyl groups and the aromatic ring, corresponding to 26 NIPAM units per DOMA unit. GPC was conducted after polymerization of the NIPAM block by taking a sample from the reaction mixture resulting in an apparent  $M_n$  of 22 200 g mol<sup>−1</sup> with  $D = 2.0$  (Fig. S4†), corresponding to a DP of *ca.* 200, from which we derive that the DOMA block length had *ca.* 8 monomer units (Fig. S1†). Due to the adhesive nature of the catechol groups, GPC was only possible before the addition of DOMA in the second step.

To confirm the chain extension of PNIPAM after DOMA addition, <sup>1</sup>H DOSY NMR was conducted (Fig. S3†).<sup>21</sup> From the DOSY spectrum, we concluded that both the resonances of DOMA and NIPAM monomers exhibited a similar diffusion coefficient, indicating successful chain extension and the formation of a block copolymer. Through turbidity measurements, the cloud point of the copolymer was determined to be



**Scheme 1** Schematic representation of the synthesis, surface-coating, and envisioned surface structure of the PNIPAM-*b*-PDOMA block copolymer using the catechol anchoring sites.





**Scheme 2** Synthesis of block copolymers: (a) synthesis of PNIPAM-*b*-PDOMA and (b) PDOMA-*b*-POEGMA by sequential RAFT polymerization.

$33.1 \pm 0.9$  °C in distilled water (Fig. S5†), which is in the range of 30–40 °C of PNIPAM copolymers.<sup>17</sup>

The block copolymers were deposited on different substrates. First, silicon substrates were coated with 120  $\mu$ L of a 2 wt% solution of the respective block copolymer in ethanol (drop-cast from a glass pipette). After drop-casting and evaporation of the solvent, a coating of  $900 \pm 30$  nm for PNIPAM-*b*-PDOMA and  $650 \pm 50$  nm for PDOMA-*b*-POEGMA was obtained as determined from AFM in the tapping mode (Fig. S6†). As plant leaves have hydrophobic surfaces with waxy cuticles, we investigated the water harvesting abilities of the block copolymer coatings on a PE model substrate. Catechol units had been shown in our previous studies to be capable of anchoring polymers to the very hydrophobic and normally inert surface of PE.<sup>20</sup> Contact angle data for the PE coated with PNIPAM-*b*-PDOMA are  $82 \pm 10$ ° for the uncoated substrate and  $45 \pm 7$ ° for the coated substrate, clearly indicating increased hydrophilicity. The coated PE substrates were placed overnight in a glass chamber through which a 100% RH airflow is blown (Fig. S7†). The adsorbed water is measured by weighing the substrates before and after their time in the chamber. The uncoated substrate collected almost no water, *i.e.* a value of  $2.2 \pm 2.0$  mg was measured (condensation of water was observed on the hydrophilic glass chamber but not on the bare hydrophobic PE substrates). In contrast, the PE substrate coated with PNIPAM-*b*-PDOMA showed an increased water uptake of  $26.9 \pm 6.6$  mg. This behavior was maintained over at least five repetitive measurements without degradation of the coating performance, which are plotted in Fig. S8.† The coated PE also collected *ca.* 1.5 mL of excess water, which was dripping from the coating during the experiment into the petri-dish below, which was not observed for the uncoated PE substrate. This confirms that the coating can harvest water from air. If we assume 1.5 mL per  $25 \text{ cm}^2$  per 15 hours, we get  $0.004 \text{ mL h}^{-1} \text{ cm}^{-2}$  for the coating. Assuming 8 hours of low temperature, *i.e.* hydrophilic state of the coating, per day and  $500 \text{ cm}^2$  surface area

per corn leaf at 18 leaves per plant, we obtain *ca.* 16 mL of water harvested per leaf and *ca.* 290 mL per plant during a humid night. While the number is obtained from an ideal situation of 100% RH in a closed system, it does give a useful indication towards the potential of the material.

For the deposition of the coating on leaves, the method and concentration are the same as used for the silicon wafers for AFM step-height measurements. The first step was to characterize the leaves and the coating using FTIR (Fig. 1). The spectra correspond to uncoated (top) and coated (middle) leaves, as well as the coating (bottom). From Fig. 1 it is apparent that the spectrum of the coated leaves shows both vibrations of the polymer and the components of the leaf.

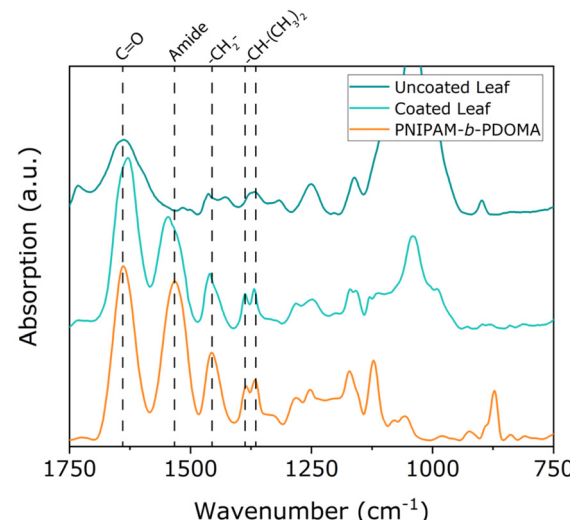


**Fig. 1** FTIR absorbance spectra of uncoated (top) and coated (middle) leaves, as well as the coating itself (bottom). Note the composite nature of the spectrum of the coated leaf, showing peaks from the leaf itself, but also the presence of peaks characteristic of the coating.



Briefly, we see peaks at  $1640\text{ cm}^{-1}$  corresponding to the  $\text{C}=\text{O}$  bond absorbances, at  $1530\text{ cm}^{-1}$  corresponding to the amide absorbances, and at  $1450\text{ cm}^{-1}$  corresponding to the hydrocarbon/alkane absorbances, and the  $1390\text{--}1360\text{ cm}^{-1}$  double peak corresponding to the isopropyl group absorbances of PNIPAM.

An important feature of the envisioned coating is rain fastness. To achieve adhesion to the leaf, we used PDOMA as an anchoring block. To confirm the adhesive capacity of these DOMA units to the leaf surface against rain, we compared the block-copolymer's adhesion with that of a homopolymer of PNIPAM on a leaf. Two leaves were coated with the respective polymers, and we performed static contact angle (SCA) measurements before and after washing with water (Fig. 2) without changing the temperature. The contact angles on plant leaves should be regarded only roughly due to the inherent roughness and inhomogeneity of the leaves. In Fig. 2A and B, we find relatively low and high contact angles, respectively, for a PNIPAM coating, without DOMA. This indicates uneven surface coverage due to the poor wetting behavior of the homopolymer. After extensive washing, see Fig. 2C, only higher contact angles can be measured. When DOMA is included in the polymer, low contact angles are obtained, even after washing with water. This means that the addition of DOMA units in the polymer structure supports adhesion, but its presence is also crucial to keep the coating in place.

At room temperature PNIPAM-*b*-PDOMA should be hydrophilic, as its temperature is below its LCST, *vs.* the hydrophobic leaf on which the coating is placed. Another set of SCA measurements are given in Fig. 3. From left to right, we show the contact angle of leaves without coating, with coating under

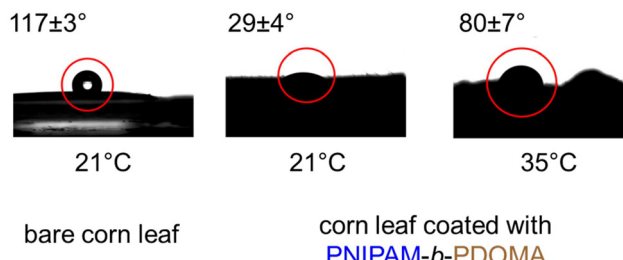


Fig. 3 Water contact angle measurements of corn leaves: left: bare corn leave at room temperature, middle and right: PNIPAM-*b*-PDOMA-coated corn leaves below and above the cloud point temperature of PNIPAM, resulting in a hydrophilic or hydrophobic coating.

LCST and with coating above LCST. Simply put, it demonstrates the thermoresponsive behavior of the copolymer. Below its LCST of  $32\text{ }^\circ\text{C}$ , the polymer coating shows hydrophilic behavior and when the temperature is increased to above  $32\text{ }^\circ\text{C}$ , it shows hydrophobic behavior instead. This behavior is switchable and does not impact coating stability. We note that quantitative CA data are not provided due to the significant error related to the leaf's roughness.

The same contact angle measurements were also performed on PDOMA-*b*-POEGMA coated leaves, which are shown in Fig. S9.† However, the contact angles did not change upon changing the temperature:  $43\pm 18^\circ$  at room temperature and  $46\pm 12^\circ$  at  $50\text{ }^\circ\text{C}$ . During these measurements, we found that water droplets washed away the PDOMA-*b*-POEGMA coating. Most likely, the volume/mass fraction of POEGMA compared to PDOMA in the block copolymer was too high for efficient

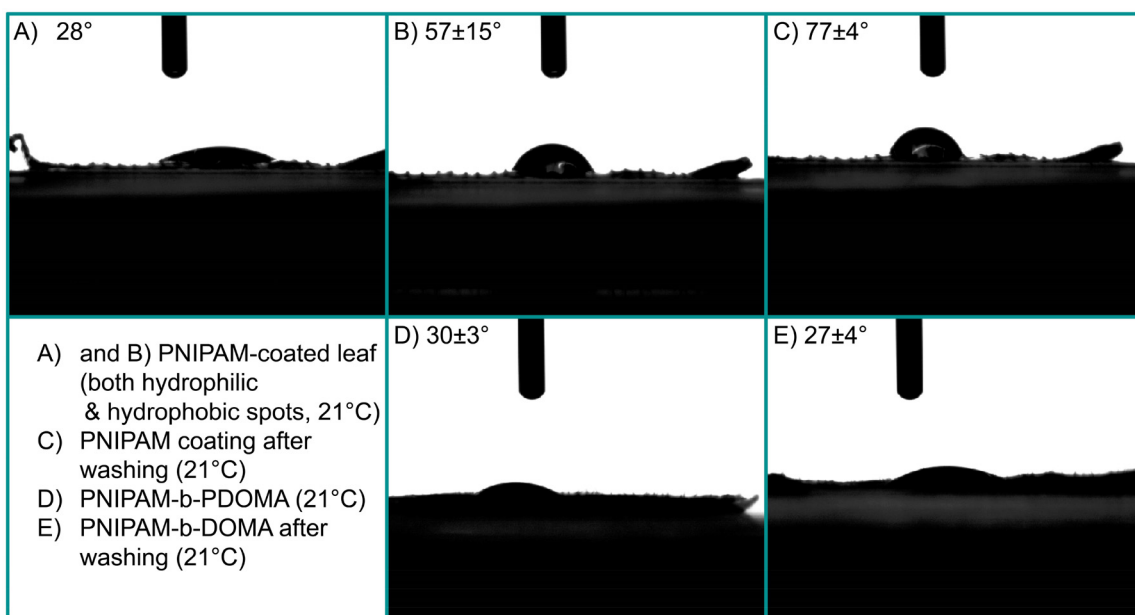
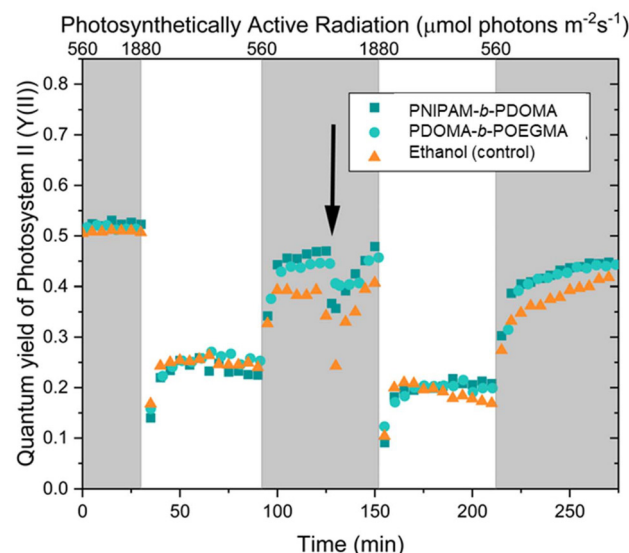


Fig. 2 Contact angle photographs of a PNIPAM coating (A–C) and a PNIPAM-*b*-PDOMA coating (bottom row). The PNIPAM coating could be removed easily by washing with water (C). The copolymer coating showed clear hydrophilic behavior at room temperature before and after washing (D and E).



coating adhesion by the catechol groups. Simple characterization of the interference of the coating with natural processes of the leaf was performed by coating the top side of the leaves with the copolymer and comparing it with a clean leaf and one coated with grease. The silicon grease coating, normally on both sides, is commonly used as a reference for interference in natural leaf behavior as it infiltrates the stomata and prevents normal transpiration from taking place.<sup>22</sup> Nonetheless, the top side of the grease-coated leaf showed the first signs of wilting (Fig. 4).

Fig. 4 presents a comparative analysis of leaves coated with the synthesized copolymer *versus* a control group coated with silicon grease. Visual observation over a 10 day period revealed the onset of wilting in the grease-coated leaves, indicated by browning along the leaf edges. Conversely, leaves treated with the copolymer exhibited no signs of wilting, suggesting that the coating does not impede normal leaf function. To corroborate this initial assessment, a comprehensive characterization of the photosynthetic process was conducted. To assess the impact of the copolymer coating on leaf photosynthesis, we conducted photosynthetic induction experiments. Leaves were transitioned from sub-saturating to saturating irradiance levels, triggering rubisco activation and stomatal opening, thereby maximizing photosynthetic activity. This protocol was performed twice: initially on uncoated leaves and subsequently on leaves coated with either the copolymer or a control substance (ethanol, the polymer solvent). Photosystem II quantum yield ( $Y_{(II)}$ ), an indicator of linear electron transport in photosynthesis, was monitored throughout the experiment (Fig. 5). Initial induction responses were similar across all leaves. However, application of the copolymer, ethanol, or silicon grease resulted in a transient decrease in  $Y_{(II)}$  (Fig. 5, black arrow), followed by recovery within 20–30 minutes. Subsequent inductions exhibited slightly lower  $Y_{(II)}$  values for all treatments, including the ethanol control. The acute, transient decrease in  $Y_{(II)}$  post-application was consistent across all treatments, suggesting that this effect was primarily attributable to



**Fig. 5** Repeated photosynthetic induction on maize leaves that are coated with the polymers or sprayed with an ethanol control. The quantum yield of photosystem II ( $Y_{(II)}$ ) is a measure for the amount of linear electron transport for photosynthesis. Blue–red light of two intensities were used for the induction: 560  $\mu\text{mol}$  photons per  $\text{m}^2$  per s that was sub-saturating (grey zone) for photosynthesis and 1880  $\mu\text{mol}$  photons per  $\text{m}^2$  per s saturating light (white zone). Application of the polymers and ethanol is marked by the black arrow.

ethanol exposure. Furthermore, the reduced  $Y_{(II)}$  in the secondary induction, observed across all treatments, indicates that this phenomenon was not polymer specific but rather related to either the ethanol application or the prior induction history,<sup>23</sup> potentially involving circadian rhythm influences.<sup>24</sup> These findings demonstrate that the copolymer coating does not significantly impede short-term photosynthetic activity in leaves.

### 3. Conclusion

We have described the synthesis and characterization of a thermoresponsive, bio-inspired adhesive polymer for AWH with a cloud point in water of  $33 \pm 1$  °C. The coating was applied to Si and PE model substrates, which were subsequently characterized for layer thickness as well as water harvesting properties. The coating was able to capture about 50% of its own weight in water. Application on leaves demonstrated that the polymer maintains its thermoresponsive behavior and is capable of adhering to leaves. A PDMA-b-POEGMA reference polymer was also synthesized and analyzed, but it lacked adhesive strength to adhere to leaf surfaces. Finally, photosynthesis induction experiments were also carried out to show that the coating does not harm the plants to which they are applied. The primary influence on the plant's behavior is found to be the ethanol solvent used for application, which should be changed for future experiments. To conclude, the coating can successfully harvest water,  $\sim 1 \text{ mg cm}^{-2}$ , it has

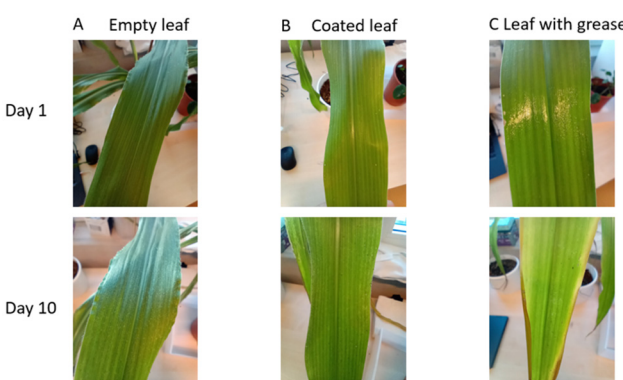


**Fig. 4** Photographs of corn plant leaves without coating (A), with coating (B), and coated with grease (C) at different points in time. The coated and uncoated leaves show similar green coloring, indicating that the leaf is still healthy, even after 10 days. The grease-coated leaf shows signs of dying, with the onset of brown edges on the leaf.



thermoreponsive switching behavior, and it does not harm the underlying plant. This proof-of-concept demonstrates the potential of our system, but continued research is needed to refine the synthesis procedures and composition for improved effectiveness. Furthermore, investigating the long-term ecological impact of these leaf-coatings in agricultural settings is crucial, with a focus on developing biodegradable alternatives currently being explored in our labs. Finally, optimizing the thermoresponsive properties will allow us to tailor this system for use in diverse environments.

## 4. Experimental

### 4.1. Materials

1,4-Dioxane (99%), 4-cyano-4-(phenylcarbonothioylthio)pentanoic acid (RAFT agent, >98%), dopamine HCl (DA, >98%), magnesium sulfate ( $\text{MgSO}_4$ , >97%), methacrylic anhydride (>94%), poly(ethylene glycol) methyl ether methacrylate (PEGMA), sodium bicarbonate (>99.7%), sodium hydroxide ( $\text{NaOH}$ , >98%), sodium tetraborate decahydrate (>99.5%) and sulfuric acid (ACS Reagent, 95%–97%) were bought from Sigma. Azobisisobutyronitrile (AIBN) and hydrogen peroxide ( $\text{H}_2\text{O}_2$ , 30%) were obtained from Merck. Ethyl acetate (Analar Rectapur, 99.9%), heptane (GPR Rectapur, >99%), *n*-hexane (GPR Rectapur, 98%), and tetrahydrofuran (GPR Rectapur, 99%) were purchased from VWR. Diethyl ether (99%) was obtained from Boom, The Netherlands. *N*-Isopropylacrylamide (>98%) was purchased from TCI Chemicals, Belgium, and recrystallized before use.

### 4.2. PNIPAM-*b*-PDOMA and PEGMA-*b*-PDOMA block copolymer synthesis

The PNIPAM-*b*-PDOMA copolymer was synthesized by RAFT polymerization according to a protocol adapted from Luan *et al.*<sup>25</sup> Briefly, 3.96 g (35 mmol) of NIPAM, 3.28 mg (0.02 mmol) of AIBN, and 27.9 mg (0.1 mmol) of RAFT agent were added to 25 mL of dioxane in a 50 mL round-bottomed flask. This solution was purged for 30 minutes with  $\text{N}_2$  before being placed in an oil bath at 75 °C for 24 h under continuous stirring and  $\text{N}_2$  overpressure. 553 mg (2.5 mmol) of DOMA was dissolved in 10 mL of dioxane and purged for 30 minutes using  $\text{N}_2$ . After 24 h, the DOMA solution was added to the round-bottomed flask and the combined mixture was left for another 18 h at 75 °C. The polymer was precipitated into diethyl ether, redissolved in dioxane, and precipitated again into diethyl ether, before being dried at reduced pressure at 60 °C overnight.  $^1\text{H}$  NMR ( $\text{DMSO-}d_6$ , 400 MHz)  $\delta$  = 8.8–8.65 (–OH, d, 2H),  $\delta$  = 6.65–6.40 (aromatic, m, 3H),  $\delta$  = 3.85 ( $\text{CH}$ , s, 1H),  $\delta$  = 1.98 (–CH–, s, 1H),  $\delta$  = 1.45 (–CH<sub>2</sub>–, s, 2H),  $\delta$  = 1.05 (–CH<sub>3</sub>, s, 6H).

For the POEGMA-*b*-PDOMA copolymer, same procedure was used except that PDOMA (2.5 mmol, 553.1 mg) was first polymerized for 18 hours and POEGMA (35 mmol, 16.2 mL in 10 mL dioxane) was added in the second step, after which the solution was left to polymerize for 24 hours.

### 4.3. Coating application

The respective polymer was dissolved at 2 wt% in ethanol and applied to surfaces using a pipette in air at 120  $\mu\text{L}$  per  $\text{cm}^2$ .

### 4.4. Atmospheric water harvesting

A PE substrate ( $5 \times 5 \text{ cm}^2$ ) was coated with 3 mL of a 2 wt% ethanol solution of PNIPAM-*b*-PDOMA. This sample was dried in air before use in the AWH experiments. For control, an uncoated PE substrate of the same dimensions was used. After weighing, the substrate was placed on a glass holder in a glass Petri dish inside a desiccator. The desiccator was connected to an inlet, outlet, and humidity sensor. Air with 100% relative humidity (RH) was blown through the inlet into the desiccator. To obtain the 100% RH air, air was blown through a bubbler in a glass column filled with water. This column was heated slightly at 35 °C to obtain 100% RH. The measurement lasted 16 hours.

$^1\text{H}$ -NMR and DOSY NMR were performed using a 400 MHz Bruker AVANCE III AMX system in  $\text{DMSO-}d_6$ .

### 4.5. Contact angle measurements

Static contact angles were measured using an OCA15 device equipped with an electronic syringe unit (Dataphysics Instruments GmbH, Germany). MilliQ water was used as the probe liquid. At least 3 measurements per sample were performed and averaged.

### 4.6. FTIR spectroscopy

FTIR spectra were obtained with a Bruker Alpha FTIR spectrometer equipped with a Platinum ATR single reflection crystal (Bruker Optic GmbH, Germany). Spectra were obtained in the range of 4000–400  $\text{cm}^{-1}$  with a resolution of 4  $\text{cm}^{-1}$  at 64 scans.

### 4.7. Photosynthetic induction measurements

Photosynthetic induction experiments were performed with a mini-PAM (Heinz Walz GmbH, Effeltrich, Germany) on the fifth fully expanded leaf from potted maize plants that were grown at the window side at the university during the summer of 2022. Experiments started with a 30 minute dark acclimation of the entire plant.  $F_v/F_m$  measurement was then performed by first switching on the measuring light (600 Hz, <1  $\mu\text{mol}$  photons per  $\text{m}^2$  per s, 650 nm red LED light) and after the fluorescence signal stabilized to measure  $F_0$ , the saturating pulse (180 ms, 12 000  $\mu\text{mol}$  photons per  $\text{m}^2$  per s, blue enriched halogen lamp, filtered to give  $\lambda < 710 \text{ nm}$  light) was applied to measure  $F_m$ .  $F_v/F_m$  was calculated according to formula (1).

$$\frac{F_v}{F_m} = \frac{F_m - F_0}{F_m} \quad (1)$$

After that, 580  $\mu\text{mol}$  photons per  $\text{m}^2$  per s of actinic white light at the leaf level was applied from a light panel (SL3500, PSI, Czech) for 30 minutes to bring the leaf in a steady-state.

Thereafter, saturating pulses were applied every 5 minutes to measure  $Y_{(II)}$ .  $Y_{(II)}$  was calculated according to formula (2).

$$Y_{(II)} = \frac{F'_m - F_s}{F'_m} \quad (2)$$

where  $F'_m$  is the maximum fluorescence measured during a saturating pulse in the presence of actinic light and  $F_s$  is the minimum fluorescence measured in the presence of actinic light. After 30 minutes, the intensity of the actinic light was switched to 1880  $\mu\text{mol}$  photons per  $\text{m}^2$  per s at the leaf level for 60 minutes to observe photosynthetic induction. Thereafter the actinic light was switched back to 580  $\mu\text{mol}$  photons per  $\text{m}^2$  per s and after 30 minutes, the polymer or control was applied by slow pipetting close to the leaf surface. After application, a 30 minute period of 580  $\mu\text{mol}$  photons per  $\text{m}^2$  per s was followed by another 60 minute period of 1880  $\mu\text{mol}$  photons per  $\text{m}^2$  per s to observe photosynthetic induction in the presence of the polymer or control. Finally, a 60 minute period of 580  $\mu\text{mol}$  photons per  $\text{m}^2$  per s of actinic light was used to follow the recovery after high light intensity treatment in the presence of the polymer or control. All experiments were started at 11:00 in the morning to prevent large diurnal effects on the measurements.

## Data availability

The data supporting this article have been included as part of the ESI.†

## Conflicts of interest

There are no conflicts to declare.

## Acknowledgements

The authors thank Ramon ten Elshof (UT) and Clemens Padberg (UT) for analyses. The authors thank the Dutch Polymer Institute (project 823t19) and the University of Twente for funding and support.

## References

- 1 R. M. Rivero, R. Mittler, E. Blumwald and S. I. Zandalinas, Developing Climate-resilient Crops: Improving Plant Tolerance to Stress Combination, *Plant J.*, 2022, **109**(2), 373–389, DOI: [10.1111/tpj.15483](https://doi.org/10.1111/tpj.15483).
- 2 D. Reay, C. Sabine, P. Smith and G. Hymus, Spring-Time for Sinks, *Nature*, 2007, **446**(7137), 727–728, DOI: [10.1038/446727a](https://doi.org/10.1038/446727a).
- 3 S. Compant, M. G. A. Van Der Heijden and A. Sessitsch, Climate Change Effects on Beneficial Plant-Microorganism Interactions: Climate Change and Beneficial Plant-Microorganism Interactions, *FEMS Microbiol. Ecol.*, 2010, **73**(2), 197–214, DOI: [10.1111/j.1574-6941.2010.00900.x](https://doi.org/10.1111/j.1574-6941.2010.00900.x).
- 4 Food Security and Food Production Systems, in *Climate Change 2014 Impacts, Adaptation, and Vulnerability*, ed. C. B. Field, V. R. Barros, D. J. Dokken, K. J. Mach and M. D. Mastrandrea, Cambridge University Press, Cambridge, 2014, pp. 485–534. DOI: [10.1017/CBO9781107415379.012](https://doi.org/10.1017/CBO9781107415379.012).
- 5 D. K. Ray, N. D. Mueller, P. C. West and J. A. Foley, Yield Trends Are Insufficient to Double Global Crop Production by 2050, *PLoS One*, 2013, **8**(6), e66428, DOI: [10.1371/journal.pone.0066428](https://doi.org/10.1371/journal.pone.0066428).
- 6 A. Raza, A. Razzaq, S. Mahmood, X. Zou, X. Zhang, Y. Lv and J. Xu, Impact of Climate Change on Crops Adaptation and Strategies to Tackle Its Outcome: A Review, *Plants*, 2019, **8**(2), 34, DOI: [10.3390/plants8020034](https://doi.org/10.3390/plants8020034).
- 7 S. Chaudhry and G. P. S. Sidhu, Climate Change Regulated Abiotic Stress Mechanisms in Plants: A Comprehensive Review, *Plant Cell Rep.*, 2022, **41**(1), 1–31, DOI: [10.1007/s00299-021-02759-5](https://doi.org/10.1007/s00299-021-02759-5).
- 8 O. Gideon Onyekachi, O. Ogbonnaya Boniface, N. Felix Gemlack and N. Nicholas, The Effect of Climate Change on Abiotic Plant Stress: A Review, in *Abiotic and Biotic Stress in Plants*, ed. A. Bosco De Oliveira, IntechOpen, 2019. DOI: [10.5772/intechopen.82681](https://doi.org/10.5772/intechopen.82681).
- 9 X. Liu, D. Beysens and T. Bourouina, Water Harvesting from Air: Current Passive Approaches and Outlook, *ACS Mater. Lett.*, 2022, **4**(5), 1003–1024, DOI: [10.1021/acsmaterialslett.1c00850](https://doi.org/10.1021/acsmaterialslett.1c00850).
- 10 X. Zhou, H. Lu, F. Zhao and G. Yu, Atmospheric Water Harvesting: A Review of Material and Structural Designs, *ACS Mater. Lett.*, 2020, **2**(7), 671–684, DOI: [10.1021/acsmaterialslett.0c00130](https://doi.org/10.1021/acsmaterialslett.0c00130).
- 11 H. Kim, S. Yang, S. R. Rao, S. Narayanan, E. A. Kapustin, H. Furukawa, A. S. Umans, O. M. Yaghi and E. N. Wang, Water Harvesting from Air with Metal-Organic Frameworks Powered by Natural Sunlight, *Science*, 2017, **356**(6336), 430–434, DOI: [10.1126/science.aam8743](https://doi.org/10.1126/science.aam8743).
- 12 F. Zhao, X. Zhou, Y. Liu, Y. Shi, Y. Dai and G. Yu, Super Moisture-Absorbent Gels for All-Weather Atmospheric Water Harvesting, *Adv. Mater.*, 2019, **31**(10), 1806446, DOI: [10.1002/adma.201806446](https://doi.org/10.1002/adma.201806446).
- 13 G. Yilmaz, F. L. Meng, W. Lu, J. Abed, C. K. N. Peh, M. Gao, E. H. Sargent and G. W. Ho, Autonomous Atmospheric Water Seeping MOF Matrix, *Sci. Adv.*, 2020, **6**(42), eabc8605, DOI: [10.1126/sciadv.abc8605](https://doi.org/10.1126/sciadv.abc8605).
- 14 X. Wang, D. Yang, M. Zhang, Q. Hu, K. Gao, J. Zhou and Z.-Z. Yu, Super-Hygroscopic Calcium Chloride/Graphene Oxide/Poly(N-Isopropylacrylamide) Gels for Spontaneous Harvesting of Atmospheric Water and Solar-Driven Water Release, *ACS Appl. Mater. Interfaces*, 2022, **14**(29), 33881–33891, DOI: [10.1021/acsami.2c08591](https://doi.org/10.1021/acsami.2c08591).
- 15 Q. Ma and X. Zheng, Preparation and Characterization of Thermo-Responsive Composite for Adsorption-Based Dehumidification and Water Harvesting, *Chem. Eng. J.*, 2022, **429**, 132498, DOI: [10.1016/j.cej.2021.132498](https://doi.org/10.1016/j.cej.2021.132498).



16 A. S. Ranganath, V. Anand Ganesh, K. Sopiha, R. Sahay and A. Baji, Investigation of Wettability and Moisture Sorption Property of Electrospun Poly(N-Isopropylacrylamide) Nanofibers, *MRS Adv.*, 2016, **1**(27), 1959–1964, DOI: [10.1557/adv.2016.164](https://doi.org/10.1557/adv.2016.164).

17 K. Jain, R. Vedarajan, M. Watanabe, M. Ishikiriyama and N. Matsumi, Tunable LCST Behavior of Poly(N-Isopropylacrylamide/Ionic Liquid) Copolymers, *Polym. Chem.*, 2015, **6**(38), 6819–6825, DOI: [10.1039/C5PY00998G](https://doi.org/10.1039/C5PY00998G).

18 Corn 2023 World Production. <https://ipad.fas.usda.gov/cropexplorer/cropview/commodityView.aspx?cropid=0440000> (accessed 2024-03-07).

19 H. Lee, B. P. Lee and P. B. Messersmith, A Reversible Wet/Dry Adhesive Inspired by Mussels and Geckos, *Nature*, 2007, **448**(7151), 338–341, DOI: [10.1038/nature05968](https://doi.org/10.1038/nature05968).

20 R. Milatz, J. Duvigneau and G. J. Vancso, Dopamine-Based Copolymer Bottlebrushes for Functional Adhesives: Synthesis, Characterization, and Applications in Surface Engineering of Antifouling Polyethylene, *ACS Appl. Mater. Interfaces*, 2023, **15**, 34023–34030, DOI: [10.1021/acsami.3c05124](https://doi.org/10.1021/acsami.3c05124).

21 P. Groves, Diffusion Ordered Spectroscopy (DOSY) as Applied to Polymers, *Polym. Chem.*, 2017, **8**(44), 6700–6708, DOI: [10.1039/C7PY01577A](https://doi.org/10.1039/C7PY01577A).

22 H. M. Duarte, I. Jakovljevic, F. Kaiser and U. Lüttge, Lateral Diffusion of CO<sub>2</sub> in Leaves of the Crassulacean Acid Metabolism Plant Kalanchoë Daigremontiana Hamet et Perrier, *Planta*, 2005, **220**(6), 809–816, DOI: [10.1007/s00425-004-1398-z](https://doi.org/10.1007/s00425-004-1398-z).

23 A. Matuszyńska, S. Heidari, P. Jahns and O. Ebenhöh, A Mathematical Model of Non-Photochemical Quenching to Study Short-Term Light Memory in Plants, *Biochim. Biophys. Acta, Bioenerg.*, 2016, **1857**(12), 1860–1869, DOI: [10.1016/j.bbabi.2016.09.003](https://doi.org/10.1016/j.bbabi.2016.09.003).

24 W. Suwannarut, S. Vialet-Chabrand and E. Kaiser, Diurnal Decline in Photosynthesis and Stomatal Conductance in Several Tropical Species, *Front. Plant Sci.*, 2023, **14**, 1273802, DOI: [10.3389/fpls.2023.1273802](https://doi.org/10.3389/fpls.2023.1273802).

25 B. Luan, B. W. Muir, J. Zhu and X. Hao, A RAFT Copolymerization of NIPAM and HPMA and Evaluation of Thermo-Responsive Properties of Poly(NIPAM-Co-HPMA), *RSC Adv.*, 2016, **6**(92), 89925–89933, DOI: [10.1039/C6RA22722H](https://doi.org/10.1039/C6RA22722H).

